



Fluorescence excitation spectroscopy of the $\tilde{A}^1A'' \leftarrow \tilde{X}^1A'$ system of jet-cooled HCCl in the region 5150–6050 Å

H. Fan, I. Ionescu, C. Annesley, J. Cummins, M. Bowers, and S.A. Reid*

Department of Chemistry, Marquette University, Milwaukee, WI 53201, USA

Received 26 November 2003; in revised form 3 February 2004

Abstract

We report new measurements of the laser induced fluorescence spectra of the HCCl $\tilde{A}^1A'' \leftarrow \tilde{X}^1A'$ system in the 5150–6150 Å region, obtained under jet-cooled conditions using a pulsed discharge source. The pure bending states $(0, \nu_2, 0)$ with $\nu_2 = 5-8$ and combination states $(0, \nu_2, \nu_3)$ with $\nu_2 = 4-6$ and $\nu_3 = 1, 2$ have been measured and the rotational structure fit to a asymmetric top rotational Hamiltonian, which yielded precise values for the band origins and effective rotational constants. Fluorescence lifetimes were measured for rotational levels in each band.

© 2004 Elsevier Inc. All rights reserved.

Keywords: Fluorescence excitation spectroscopy of HCCl; Fluorescence lifetime of HCCl

1. Introduction

Carbenes have been well studied both experimentally and theoretically due to their importance in chemistry [1–12]. While methylene has a triplet ground state [1, 11], it is well known that halogen substitution stabilizes the singlet state via back-donation of electron density from the halogen to the empty out-of-plane carbon $2p$ orbital, and thus the smaller mono-halocarbenes (HCF, HCCl, and HCB) exhibit singlet ground states [4–10]. As one of the important simple carbenes, HCCl has received significant attention [10, 13–18].

The ground (\tilde{X}^1A') state of HCCl forms a Renner–Teller pair with \tilde{A}^1A'' . Merer and Travis (MT) reported the rotationally resolved absorption spectrum for the HCCl $\tilde{A}^1A'' \leftarrow \tilde{X}^1A'$ system in the region 5500–8200 Å [10], and assigned the pure bending states $(0, \nu_2, 0)$ for HCCl ($\nu_2 = 1-6$) and DCCl ($\nu_2 = 0-9$). The barrier to linearity in the excited state was determined to lie $\sim 2250 \text{ cm}^{-1}$ above the vibrationless level, and all sub-bands with $K'_a \geq 1$ were very weak and severely perturbed. Subsequently, Hirota and co-workers [13, 14]

reported the dye laser excitation spectrum of $\tilde{A}^1A''(050) \leftarrow \tilde{X}^1A'(000)$ at Doppler-limited resolution. Consistent with the findings of MT, the spectrum showed only excited state sub-bands with $K'_a = 0$, and rotational perturbations were observed in this sub-band for high J levels. More recently, high resolution spectra of $\tilde{A}^1A''(000)$ and $\tilde{A}^1A''(010)$ were obtained by Sears and co-workers [15, 16], where the geometry of HCCl in the excited state was explored, the barrier to linearity re-evaluated and the dependence of excited state perturbations on K'_a and J investigated. The dispersed fluorescence spectrum of the HC^{35}Cl and $\text{DCCl } \tilde{A}^1A'' \rightarrow \tilde{X}^1A'$ transition was also recently reported [17, 18].

In this article, we report new measurements on the fluorescence excitation spectrum of the HCCl $\tilde{A}^1A'' \leftarrow \tilde{X}^1A'$ system, focusing on bands with $\nu_2 \geq 6$. In addition, we report the fluorescence lifetimes of bands in this system for the first time.

2. Experimental section

The apparatus and high voltage pulsed discharge nozzle have been previously described [19, 20]. Briefly, HCCl was produced by a pulsed discharge (800–1200 V pulse, 10–50 μs duration, <1 mA current level) through

* Corresponding author. Fax: 1-414-288-7066.
E-mail address: scott.reid@mu.edu (S.A. Reid).

a $\sim 2\%$ $\text{CH}_2\text{Cl}_2/\text{Ar}$ mixture expanded at a typical backing pressure of 2 atm. The timing of laser, nozzle, and discharge firing was controlled by a digital delay generator. The laser system was an etalon narrowed dye laser (Lambda-Physik Scanmate 2E) operating on Rhodamine 6G, Rhodamine B or Coumarin series (C153, C307) dye, pumped by the third harmonic of an Nd:YAG laser (Continuum Powerlite 7010 or NY61). The laser beam entering the chamber was not focused, with typical pulse energy of $\sim 500 \mu\text{J}$ and diameter of $\sim 3 \text{ mm}$. A quartz window was used to introduce a portion of the dye laser fundamental into an Fe–Ne or Fe–Ar hollow cathode lamp for absolute wavelength calibration. For spectroscopic measurements, the laser beam, molecular beam and detector were mutually perpendicular, while for lifetime measurements the molecular beam was oriented at 180° to the detector in order to minimize fly-out from the detector field of view. An appropriate long-pass cut-off filter was used to block the scattered laser light, and fluorescence was imaged by $f/2.4$ collection optics onto a photomultiplier tube detector typically held at -600 V .

For the spectral scan, a ‘fast scan’ mode was used, where 10 shots were averaged in the baseline range and 30 shots were collected on the peaks. The peak positions were determined by fitting to a Gaussian lineshape function. For lifetime measurements, the signal was terminated into 50Ω and digitized at a typical sampling rate of 250 MHz. The waveforms were averaged over 2000 laser shots and five decays were individually fit,

with the reported lifetime the average of those measurements.

3. Results and discussion

A spectrum of the $\text{HCCl } \tilde{A} \leftarrow \tilde{X}$ system in the region of the (0,6,0), (0,5,1), and (0,4,2) bands is shown in Fig. 1. Consistent with previous work [10,13,14], only excited state levels with $K'_a = 0$ appear with significant intensity for both HC^{35}Cl and HC^{37}Cl , including the nominally forbidden qQ_0 sub-band, which arises from axis-switching due to the large change in equilibrium angle upon electronic excitation [10]. The observed bands are largely free from rotational perturbations for the range of J accessed under our experimental condi-

Table 1
Band origins and rotational constants (in cm^{-1}) for the HC^{35}Cl bands measured in this work

Level	Band origin (cm^{-1})	$(B + C)/2$	N^a	σ^b
050	16590.516(22)	0.606(1)	12	0.016
041	16647.694(43)	0.604(4)	13	0.035
060	17465.713(54)	0.599(2)	12	0.040
051	17526.414(43)	0.610(2)	12	0.032
042	17571.650(40)	0.602(2)	13	0.030
070	18398.141(66)	0.591(1)	12	0.013
061	18448.840(18)	0.588(6)	13	0.013
080	19255.663(42)	0.580(1)	15	0.034

^a Number of lines used in fit.

^b Standard deviation of fit.

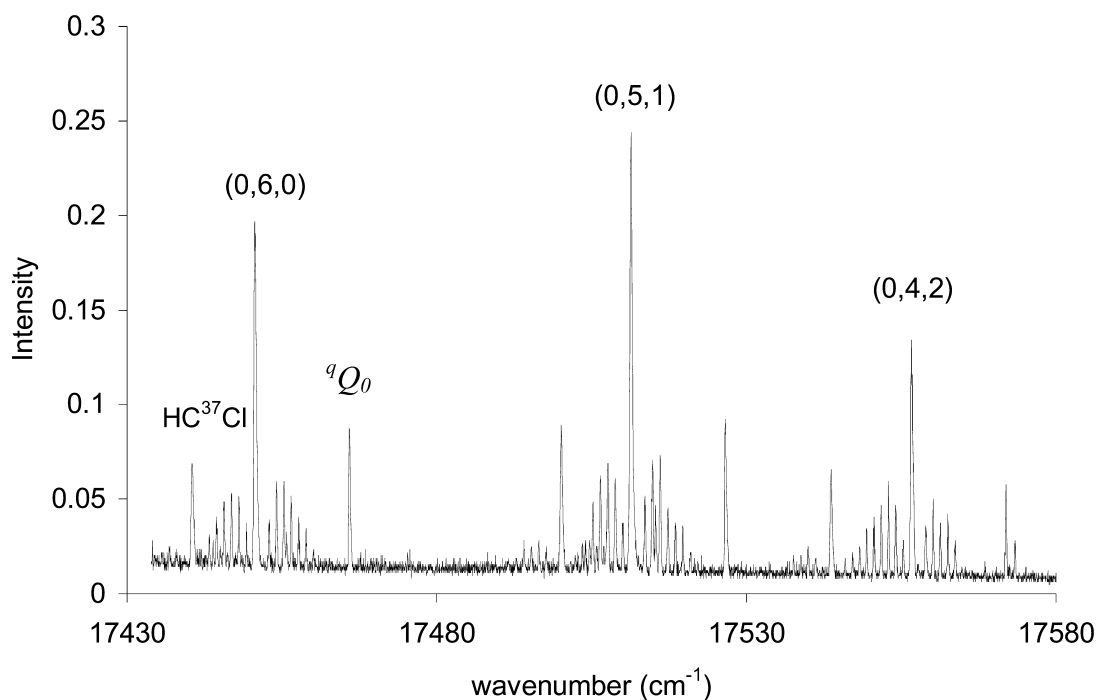


Fig. 1. Fluorescence excitation spectrum of the $\tilde{A}^1A'' \leftarrow \tilde{X}^1A'$ system of HCCl in the region of the (0,6,0), (0,5,1), and (0,4,2) bands. Assignments are noted.

Table 2
Transitions included in the fits for each band and the fit residuals

Transitions	Observed (cm ⁻¹)	Calculated (cm ⁻¹)	Intensity	Observed– Calculated (cm ⁻¹)
HCCl $\tilde{A}^1A''(0,5,0)$				
6 ₀₆ ← 7 ₁₆	16567.278	16567.250	0.007	0.028
5 ₀₅ ← 6 ₁₅	16568.364	16568.366	0.016	-0.002
4 ₀₄ ← 5 ₁₄	16569.486	16569.497	0.031	-0.011
2 ₀₂ ← 3 ₁₂	16571.822	16571.799	0.039	0.023
1 ₀₁ ← 2 ₁₁	16572.980	16572.971	0.044	0.009
0 ₀₀ ← 1 ₁₀	16574.138	16574.755	0.030	-0.017
2 ₀₂ ← 1 ₁₀	16577.777	16577.788	0.035	-0.011
3 ₀₃ ← 2 ₁₁	16579.025	16579.025	0.041	-0.004
4 ₀₄ ← 3 ₁₂	16580.271	16580.276	0.049	-0.005
5 ₀₅ ← 4 ₁₃	16581.549	16581.540	0.031	0.009
6 ₀₆ ← 5 ₁₄	16582.820	16582.817	0.025	0.003
7 ₀₇ ← 6 ₁₅	16584.087	16584.109	0.013	-0.022
HCCl $\tilde{A}^1A''(0,4,1)$				
5 ₀₅ ← 6 ₁₅	16625.449	16625.511	0.026	-0.062
4 ₀₄ ← 5 ₁₄	16626.598	16626.653	0.016	-0.055
3 ₀₃ ← 4 ₁₃	16627.780	16627.806	0.025	-0.026
2 ₀₂ ← 3 ₁₂	16628.966	16628.971	0.024	-0.005
1 ₀₁ ← 2 ₁₁	16630.140	16630.146	0.027	-0.006
0 ₀₀ ← 1 ₁₀	16631.324	16631.333	0.015	-0.009
2 ₀₂ ← 1 ₁₀	16634.990	16634.959	0.013	0.031
3 ₀₃ ← 2 ₁₁	16636.226	16636.190	0.020	0.036
4 ₀₄ ← 3 ₁₂	16637.469	16637.431	0.028	0.038
5 ₀₅ ← 4 ₁₃	16638.711	16638.684	0.019	0.027
6 ₀₆ ← 5 ₁₄	16639.979	16639.948	0.015	0.031
7 ₀₇ ← 6 ₁₅	16641.234	16641.224	0.010	0.010
8 ₀₈ ← 7 ₁₆	16642.500	16642.511	0.005	-0.011
HCCl $\tilde{A}^1A''(0,6,0)$				
5 ₀₅ ← 6 ₁₅	17443.338	17443.370	0.021	-0.032
4 ₀₄ ← 5 ₁₄	17444.510	17444.565	0.023	-0.055
3 ₀₃ ← 4 ₁₃	17445.710	17445.761	0.033	-0.051
2 ₀₂ ← 3 ₁₂	17446.931	17446.957	0.037	-0.026
1 ₀₁ ← 2 ₁₁	17448.141	17448.155	0.033	-0.014
0 ₀₀ ← 1 ₁₀	17449.350	17449.352	0.017	-0.002
2 ₀₂ ← 1 ₁₀	17452.988	17452.946	0.021	0.042
3 ₀₃ ← 2 ₁₁	17454.201	17454.145	0.039	0.056
4 ₀₄ ← 3 ₁₂	17455.398	17455.344	0.042	0.054
5 ₀₅ ← 4 ₁₃	17456.566	17456.543	0.038	0.023
6 ₀₆ ← 5 ₁₄	17457.750	17457.743	0.023	0.007
7 ₀₇ ← 6 ₁₅	17458.942	17458.944	0.016	-0.002
HCCl $\tilde{A}^1A''(0,5,1)$				
5 ₀₅ ← 6 ₁₅	17504.061	17504.126	0.011	-0.065
4 ₀₄ ← 5 ₁₄	17505.269	17505.303	0.032	-0.034
3 ₀₃ ← 4 ₁₃	17506.469	17506.484	0.047	-0.015
2 ₀₂ ← 3 ₁₂	17507.667	17507.669	0.050	-0.002
1 ₀₁ ← 2 ₁₁	17508.872	17508.859	0.047	0.013
0 ₀₀ ← 1 ₁₀	17510.079	17510.053	0.024	0.026
2 ₀₂ ← 1 ₁₀	17513.649	17513.649	0.032	-0.009
3 ₀₃ ← 2 ₁₁	17514.859	17514.868	0.056	-0.009
4 ₀₄ ← 3 ₁₂	17516.102	17516.081	0.056	0.021
5 ₀₅ ← 4 ₁₃	17517.342	17517.299	0.038	0.043
6 ₀₆ ← 5 ₁₄	17518.556	17518.522	0.025	0.034
7 ₀₇ ← 6 ₁₅	17519.745	17519.748	0.025	-0.003
HCCl $\tilde{A}^1A''(0,4,2)$				
7 ₀₇ ← 8 ₁₇	17547.136	17547.103	0.022	0.033
6 ₀₆ ← 7 ₁₆	17548.272	17548.250	0.011	0.022
5 ₀₅ ← 6 ₁₅	17549.388	17549.405	0.022	-0.017
4 ₀₄ ← 5 ₁₄	17550.579	17550.568	0.023	0.011

Table 2 (continued)

Transitions	Observed (cm ⁻¹)	Calculated (cm ⁻¹)	Intensity	Observed– Calculated (cm ⁻¹)
3 ₀₃ ← 4 ₁₃	17551.728	17551.737	0.036	-0.009
2 ₀₂ ← 3 ₁₂	17552.909	17552.914	0.039	-0.005
1 ₀₁ ← 2 ₁₁	17554.092	17554.098	0.039	-0.006
0 ₀₀ ← 1 ₁₀	17555.281	17555.289	0.019	-0.008
2 ₀₂ ← 1 ₁₀	17558.937	17558.903	0.027	0.034
3 ₀₃ ← 2 ₁₁	17560.112	17560.112	0.032	-0.009
4 ₀₄ ← 3 ₁₂	17561.364	17561.346	0.025	0.018
5 ₀₅ ← 4 ₁₃	17562.593	17562.579	0.027	0.014
6 ₀₆ ← 5 ₁₄	17563.743	17563.818	0.068	-0.075
HCCl $\tilde{A}^1A''(0,7,0)$				
7 ₀₇ ← 8 ₁₇	18370.299	18370.290	0.009	0.009
6 ₀₆ ← 7 ₁₆	18371.578	18371.594	0.100	-0.016
5 ₀₅ ← 6 ₁₅	18372.893	18372.884	0.170	0.009
4 ₀₄ ← 5 ₁₄	18374.162	18374.159	0.150	0.003
3 ₀₃ ← 4 ₁₃	18375.427	18375.419	0.180	0.008
2 ₀₂ ← 3 ₁₂	18376.677	18376.664	0.190	0.013
1 ₀₁ ← 2 ₁₁	18377.902	18377.893	0.020	0.009
0 ₀₀ ← 1 ₁₀	18379.078	18379.106	0.060	-0.028
3 ₀₃ ← 2 ₁₁	18383.806	18383.803	0.014	0.003
4 ₀₄ ← 3 ₁₂	18384.935	18384.938	0.016	-0.003
5 ₀₅ ← 4 ₁₃	18386.060	18386.058	0.019	0.002
6 ₀₆ ← 5 ₁₄	18387.153	18387.162	0.020	-0.009
HCCl $\tilde{A}^1A''(0,6,1)$				
7 ₀₇ ← 8 ₁₇	18420.753	18420.766	0.008	-0.013
6 ₀₆ ← 7 ₁₆	18422.120	18422.119	0.011	0.001
5 ₀₅ ← 6 ₁₅	18423.426	18423.450	0.010	-0.024
4 ₀₄ ← 5 ₁₄	18424.755	18424.759	0.015	-0.004
3 ₀₃ ← 4 ₁₃	18426.050	18426.046	0.019	0.004
2 ₀₂ ← 3 ₁₂	18427.318	18427.311	0.013	0.007
1 ₀₁ ← 2 ₁₁	18428.558	18428.554	0.011	0.004
2 ₀₂ ← 1 ₁₀	18433.303	18433.300	0.006	0.003
3 ₀₃ ← 2 ₁₁	18434.434	18434.430	0.018	0.004
4 ₀₄ ← 3 ₁₂	18435.532	18435.538	0.012	-0.006
5 ₀₅ ← 4 ₁₃	18436.610	18436.623	0.015	-0.013
6 ₀₆ ← 5 ₁₄	18437.700	18437.686	0.018	0.014
7 ₀₇ ← 6 ₁₅	18438.750	18438.728	0.016	0.022
HCCl $\tilde{A}^1A''(0,8,0)$				
8 ₀₈ ← 9 ₁₈	19226.932	19226.944	0.006	-0.012
7 ₀₇ ← 8 ₁₇	19228.467	19228.402	0.007	0.065
6 ₀₆ ← 7 ₁₆	19229.893	19229.823	0.010	0.070
5 ₀₅ ← 6 ₁₅	19231.226	19231.208	0.013	0.018
4 ₀₄ ← 5 ₁₄	19232.556	19232.555	0.012	-0.001
2 ₀₂ ← 3 ₁₂	19233.852	19233.865	0.019	-0.013
1 ₀₁ ← 2 ₁₁	19235.116	19235.138	0.013	-0.022
0 ₀₀ ← 1 ₁₀	19236.347	19236.374	0.007	-0.027
2 ₀₂ ← 1 ₁₀	19239.835	19239.854	0.005	-0.019
3 ₀₃ ← 2 ₁₁	19240.935	19240.939	0.011	-0.004
4 ₀₄ ← 3 ₁₂	19241.993	19241.987	0.011	0.006
5 ₀₅ ← 4 ₁₃	19242.993	19242.997	0.010	-0.004
6 ₀₆ ← 5 ₁₄	19243.985	19243.969	0.008	0.016
7 ₀₇ ← 6 ₁₅	19244.875	19244.905	0.004	-0.030
8 ₀₈ ← 7 ₁₆	19245.759	19245.804	0.005	-0.045

tions. As we demonstrate below, combination bands involving C–Cl stretching excitation primarily arise from Fermi resonances with pure bending levels. The rotational structure of each observed band was fit to an asymmetric top rotational Hamiltonian using the

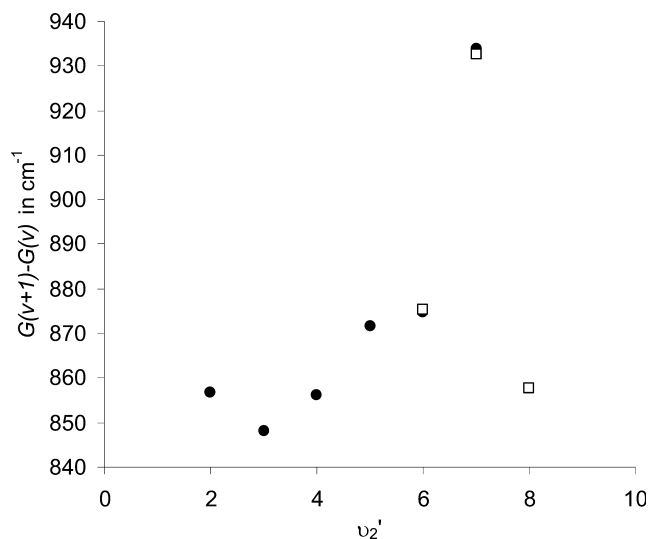


Fig. 2. Bending vibrational energy spacing [$G(v+1)-G(v)$] in the \tilde{A}^1A'' state of HCCl, plotted versus quanta of bending excitation. Legend: (\square) this work; (\bullet) Merer and Travis ([10]).

well-known ground state rotational constants [14], from which band origins and excited state effective rotational constants were derived. The fit results for HC^{35}Cl for all bands measured in this work are listed in Table 1, while Table 2 gives a complete list of the observed and calculated line positions for each band.

The dependence of the vibrational energy level spacings and rotational constants on quanta of bending excitation is shown in Figs. 2 and 3, respectively, which combine our results with those of previous authors. As shown by MT [10], and predicted earlier by Dixon [21], the bending vibrational spacings initially decrease, reaching a minimum around $(0,3,0)$, which signals the position of the barrier to linearity. Above this point, the

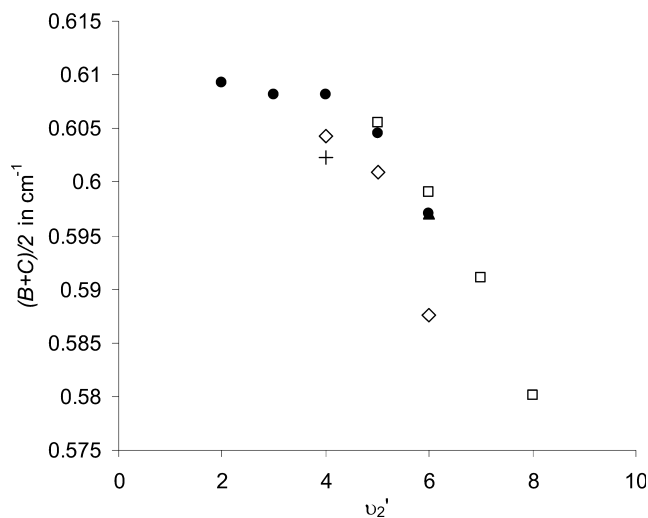


Fig. 3. Effective rotational constants [$(B+C)/2$] in the \tilde{A}^1A'' state of HCCl, plotted versus quanta of bending excitation. Legend: (\square) this work ($0, v_2', 0$); (\bullet) Merer and Travis ($0, v_2', 0$); (\diamond) this work ($0, v_2', 1$); (\blacktriangle) Merer and Travis ($0, v_2', 1$); and (+) this work ($0, v_2', 2$).

spacings increase and should eventually reach a value consistent with that of a linear molecule. Our results show a sharp decrease for $(0,8,0)$, which can be understood by considering that this level is pushed down in energy due either to Fermi resonance or another homogeneous perturbation, as our lifetime measurements indicate (see below). On the other hand, the effective rotational constant [$(B+C)/2$] decreases sharply with increasing bending quanta (Fig. 3), which reflects both the transition to linearity and, at higher energies, mixing with levels containing C–Cl stretching excitation. Note the obvious decrease in $(B+C)/2$ observed following excitation of the C–Cl stretch (Fig. 3), as shown, e.g., when comparing the series of levels $(0,4, v_3')$.

It may seem unusual that Fermi resonances among the pure bending $(0, v_2', 0)$ and combination states $(0, v_2' - 1, 1)$ and $(0, v_2' - 2, 2)$ only appear for $(0, 5, 0)$ and above, a fact first noted by MT [10]. However, this can be explained by the trend in shown in Fig. 2, namely, the energy dependence of the bending intervals, which increase with increasing v_2' above the barrier, pushing the levels into resonance.

Several studies have examined the kinetics of HCCl reactions using laser induced fluorescence [22–24]; however, to our knowledge no systematic measurement of the fluorescence lifetimes has ever been performed. The lifetimes of the bands measured in this work, averaged over rotational level, are given in Table 3, and plotted in Fig. 4 as a function of energy. In contrast to the energy dependence found for the lifetimes of $\text{HCF}(\tilde{A})$ levels with $K_a' = 0$ [21], which decrease with increasing energy as expected based on the cubic wavelength dependence, the HCCl lifetimes increase slightly with increasing energy. This must arise from a homogeneous perturbation, as the measured lifetimes show no obvious J dependence, the variation in lifetime for different rotational states being no greater than 10%. This trend is consistent with the lack of rotational perturbations in the spectra.

Explanations for the lifetime behavior include coupling to different electronic states (e.g., \tilde{a}^3A''), and/or the Fermi resonances so apparent in the spectra at higher energies (Fig. 1). In the Born–Oppenheimer

Table 3
Average fluorescence lifetimes for the HC^{35}Cl bands measured in this work

Level	Fluorescence lifetime (μs)
050	4.66(5)
041	4.93(4)
060	4.61(3)
051	4.67(4)
042	4.75(4)
070	4.93(2)
061	5.02(9)
080	5.73(17)

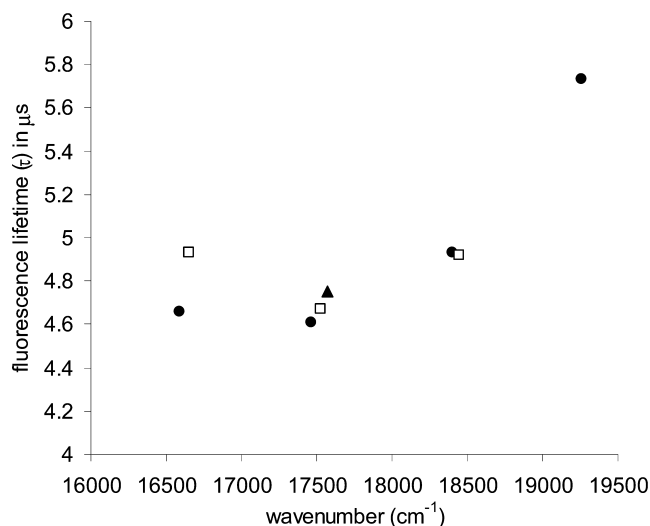


Fig. 4. Average fluorescence lifetimes for the \tilde{A}^1A'' bands measured in this work, plotted versus transition energy. Legend: ●, $(0, \nu_2', 0)$; □, $(0, \nu_2', 1)$; and ▲, $(0, \nu_2', 2)$.

approximation, all \tilde{A} state vibrational levels should exhibit a similar lifetime. However, in the case of HCF, we observe consistently longer lifetimes (by $\sim 10\%$) for the $K_a = 0$ levels of unperturbed combination states $(0, \nu_2' - 1, 1)$ compared to the pure bending levels $(0, \nu_2', 0)$ [25]. While small, this difference could explain the observed trend, with the possible exception of the much longer lifetime for $(0, 8, 0)$. Moreover, the similarity in lifetime for members of a given Fermi diad or triad (Fig. 4) is consistent with the mixed nature of these levels. At this stage, however, it is impossible to rule out coupling with other electronic states.

4. Conclusions

The fluorescence excitation spectra of HCCl bands $(0, \nu_2', \nu_3')$ of the $\tilde{A}^1A'' \leftarrow \tilde{X}^1A'$ system were measured in the region 5150–6050 Å. The line positions were fit to an asymmetric top Hamiltonian, yielding precise values for the band origins and effective rotational constants. The effective rotational constants decrease sharply with an increase in bending quanta above the barrier to linearity. At higher energies, the appearance of combination bands involving excitation in the C–Cl stretch is attributed to Fermi resonance, facilitated by the near degeneracy of the vibronic levels $(0, \nu_2', 0)$, $(0, \nu_2' - 1, 1)$ and $(0, \nu_2' - 2, 2)$. As found in previous work, sub-bands with $K_a' \geq 1$ do not appear strongly in the spectrum, a result which highlights the importance of the Renner–Teller

interaction. As the barrier to linearity in the \tilde{A}^1A'' state of HCCl is much smaller than in HCF, the onset of strong Renner–Teller effects occurs at much lower energies in the \tilde{A}^1A'' state [21].

Acknowledgments

The authors acknowledge the donors of the American Chemical Society, Petroleum Research fund for partial support of this research, and thank Ju Xin for assistance in data acquisition and analysis.

References

- [1] G. Herzberg, J.W.C. Johns, Proc. R. Soc. Lond. Ser. A. 295 (1966) 107–128.
- [2] W. Kirmse, Carbene Chemistry, Academic, New York, 1971.
- [3] G. Bertrand (Ed.), Carbene Chemistry: From Fleeting Intermediates to Powerful Reagents, Fontis Media and Marcel Dekker, The Netherlands, 2002.
- [4] H. Petek, D.J. Nesbitt, C.B. Moore, F.W. Birss, D.A. Ramsay, J. Chem. Phys. 86 (1987) 1189–1205.
- [5] E.A. Carter, W.A. Goddard III, J. Chem. Phys. 88 (1988) 1752–1763.
- [6] G.E. Scseria, M. Durán, R.G.A.R. Maclagan, H.F. Schaefer III, J. Am. Chem. Soc. 108 (1986) 3248–3253.
- [7] S.K. Shin, W.A. Goddard III, J.L. Beauchamp, J. Phys. Chem. 94 (1990) 6963–6969.
- [8] K.K. Irikura, W.A. Goddard III, J.L. Beauchamp, J. Am. Chem. Soc. 114 (1992) 48–51.
- [9] C.W. Bauschlicher Jr., H.F. Schaefer III, P.S. Bagus, J. Am. Chem. Soc. 99 (1977) 7106–7110.
- [10] A.J. Merer, D.N. Travis, Can. J. Phys. 44 (1966) 525–547.
- [11] T.J. Sears, P.R. Bunker, A.R.W. McKellar, J. Chem. Phys. 75 (1981) 4731–4732.
- [12] A.J. Merer, D.N. Travis, Can. J. Phys. 44 (1966) 1541–1550.
- [13] E. Hirota, Faraday Discuss. Chem. Soc. 74 (1981) 87–95.
- [14] M. Kakimoto, S. Saito, E. Hirota, J. Mol. Spectrosc. 97 (1983) 194–203.
- [15] B.-C. Chang, T.J. Sears, J. Chem. Phys. 102 (1995) 6347–6353.
- [16] B.-C. Chang, T.J. Sears, J. Mol. Spectrosc. 173 (1995) 391–403.
- [17] C.-W. Chen, T.-C. Tsai, B.-C. Chang, Chem. Phys. Lett. 347 (2001) 73–78.
- [18] C.-L. Lee, M.-L. Liu, B.-C. Chang, J. Chem. Phys. 117 (2002) 3263–3268.
- [19] H. Fan, I. Ionescu, C. Annesley, S.A. Reid, Chem. Phys. Lett. 378 (2003) 548–552.
- [20] J. Xin, H. Fan, I. Ionescu, C. Annesley, S.A. Reid, J. Mol. Spectrosc. 219 (2003) 37–44.
- [21] R.N. Dixon, Trans. Faraday Soc. 60 (1964) 1363–1368.
- [22] R. Wagener, H.G. Wagner, Z. Phys. Chem. 175 (1992) 9–14.
- [23] H.-H. Carstensen, C. Rehbein, H. Wagner, Ber. Bun.-Ges. Phys. Chem. 101 (1997) 1429–1432.
- [24] R.E. Baren, M.A. Erickson, J.F. Hershberger, Int. J. Chem. Kinetics 34 (2002) 12–17.
- [25] H. Fan, I. Ionescu, C. Annesley, S.A. Reid (unpublished results).